Analysis of the Impact of Remote Oxygen Plasma Treatment on the Surface Chemistry and Electrochemical Properties of Graphite Felt Electrodes for Redox Flow Batteries

L. Mauricio Murillo-Herrera[a]*, Carlos J. Mingoes[a], J. Obrero-Pérez[b], Juan R. Sánchez-Valencia[b], Michael W. Thielke[a], Ángel Barranco[b], Ana B. Jorge Sobrido[a]*.

[a]School of Engineering and Materials Science. Queen Mary University of London. Mile End Rd, London E1 4NS, United Kingdom

[b]Instituto de Ciencia de Materiales de Sevilla. Consejo Superior de Investigaciones Cientificas. c/Américo Vespucio 49, 41092, Sevilla, Spain.

Table of contents

Chemical shift		GF pristine					GF400					GF400 anomalous	P10s				P60s				
		Sample1	Sample2	Sample3	Average	STD	Sample1	Sample2	Sample3	Average	STD	Sample1	Sample1	Sample2	Sample3	Average	STD	Sample1	Sample2	Sample3	Average	STD
C1s	C=C	80.63	77.96	77.82	78.80	1.58	76.73	74.15	76.62	75.83	1.46	63.74	69.20	69.97	70.19	69.79	0.52	74.74	76.66	69.93		
	C-C low BE C-H	7.24	8.41	7.51	7.72	0.61	7.22	6.06	6.93	6.74	0.60	13.41	3.98	6.99	3.09	4.69	2.04	6.02	5.28	8.74		
	C-C high BE Adv. C	0.96	1.59	3.65	2.07	1.41	0.84	7.63	3.93	4.13	3.40	10.95	7.97	4.52	6.03	6.17	1.73	3.33	2.68	4.77		
	C-O	0.60	0.70	1.49	**0.93**	0.49	1.36	1.32	1.26	**1.31**	0.05	5.53	3.77	4.20	5.18	**4.38**	0.72	4.75	6.07	4.72		
	C=O	0.72	1.01	0.55	**0.76**	0.23	2.27	2.06	1.37	**1.90**	0.47	5.57	5.95	4.77	3.52	**4.75**	1.22	2.12	0.87	2.46		
	O-C=O	0.32	0.56	0.48	**0.45**	0.12	1.19	0.65	0.96	**0.93**	0.27	0.80	4.14	4.66	4.60	**4.47**	0.28	3.16	3.69	3.44		
	Pi-Pi*	9.52	9.78	8.51	9.27	0.67	10.38	8.12	8.93	9.14	1.15	0.00	4.99	4.89	6.65	5.51	0.99	5.87	4.74	4.87		
	Residual STD	1.51	1.07	1.20	1.26		1.60	1.01	1.26			3.33	1.11	1.25	1.16	1.17		1.38	1.38	1.07		
O1s		Sample1	Sample2	Sample3	Average	STD	Sample1	Sample2	Sample3	Average	STD	Sample1	Sample1	Sample2	Sample3	Average	STD	Sample1	Sample2	Sample3	Average	STD
	C=O	53.19	55.67	48.02	**52.29**	3.90	60.37	36.32	48.02	**48.24**	12.03	53.73	53.97	49.18	42.98	**48.71**	5.51	38.91	31.02	38.58		
	C-O aliphatic	39.78	40.64	45.62	**42.01**	3.15	33.20	61.02	45.62	**46.61**	13.94	45.80	42.10	46.23	51.58	**46.64**	4.75	58.36	66.38	54.61		
	Ads O2, H2O	6.46	3.69	6.35	**5.50**	1.57	6.42	2.66	6.32	5.13	2.14	0.48	3.93	4.59	5.43	4.65	0.75	2.74	2.61	5.81		
	Residual STD	1.16	0.95	0.96	1.02		1.07	0.94	0.91	0.97		2.47	0.92	0.99	0.83	0.91		0.88	0.92	1.01		
Regions		Sample1	Sample2	Sample3	Average	STD	Sample1	Sample2	Sample3	Average	STD	Sample 1	Sample1	Sample2	Sample3	Average	STD	Sample1	Sample2	Sample3	Average	STD
	C1s	98.34	97.73	97.47	97.85	0.45	95.17	95.92	96.48	95.86	0.54	88.33	86.20	86.39	86.67	86.42	0.24	89.96	89.40	89.38	89.58	0.24
	O1s	1.66	2.27	2.53	2.15	0.45	4.83	4.08	3.52	4.14	0.54	11.67	13.80	13.61	13.33	13.58	0.24	10.04	10.60	10.62	10.42	0.24

XPS analysis.

Table S1: Deconvolution of High resolution XPS data

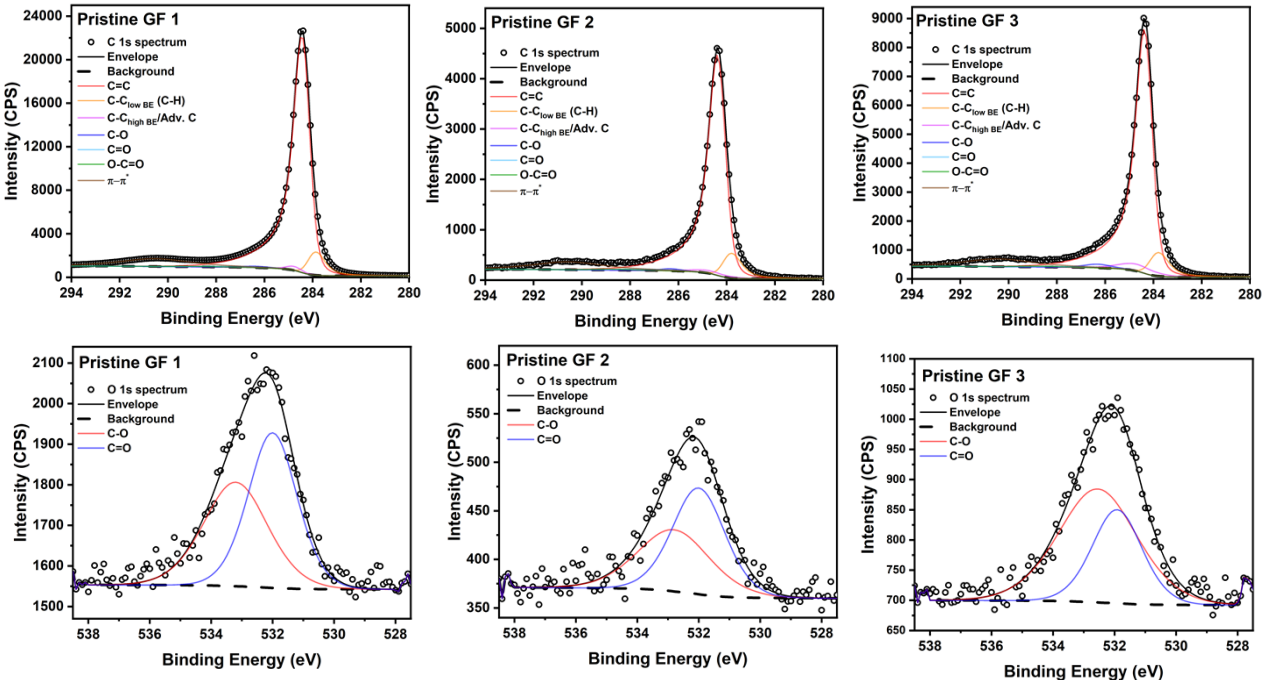

Figure S1: Pristine **GF** high resolution C1s & O1s spectra.

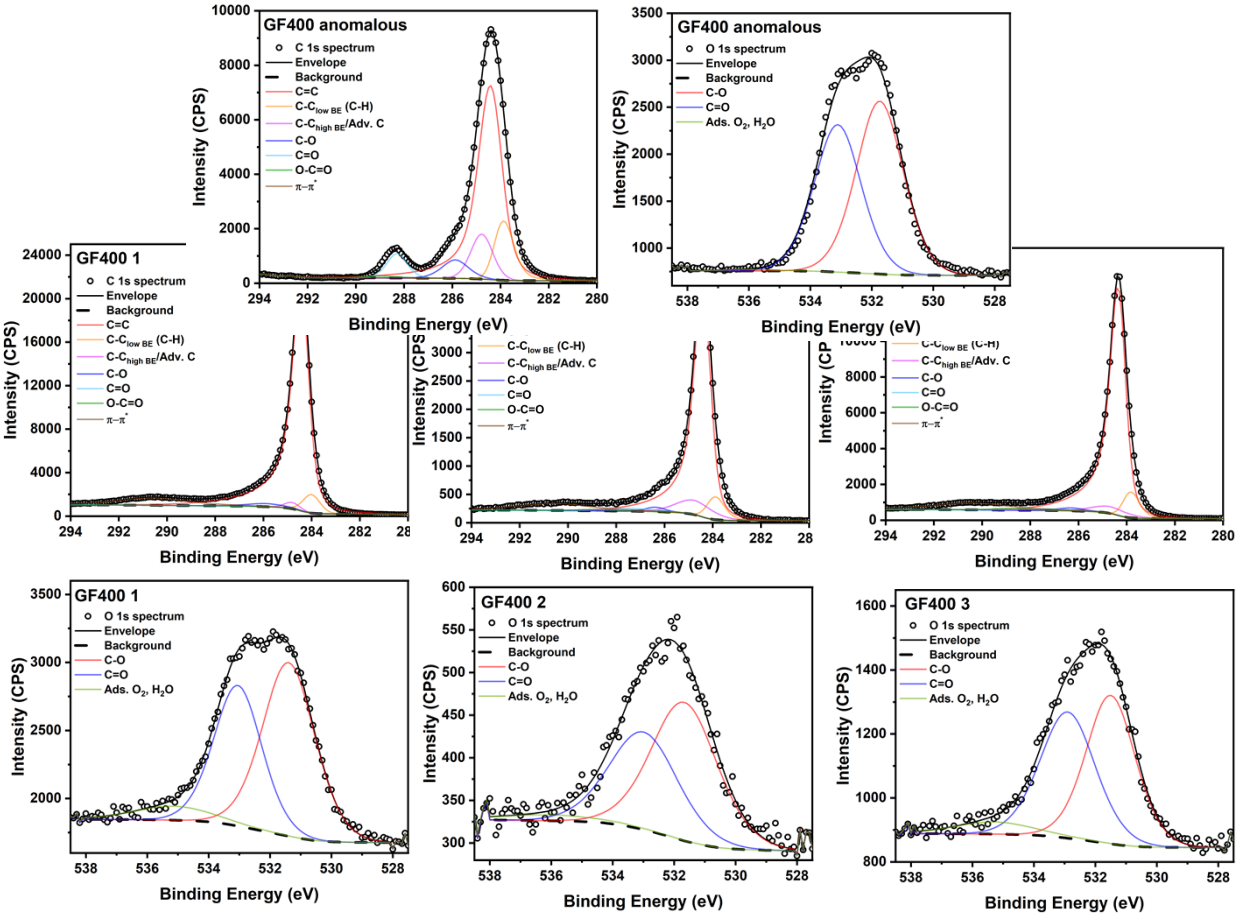

Figure S2: **GF400** high resolution C1s & O1s spectra.

Figure S3: Anomalous **GF400** high resolution C1s & O1s spectra.

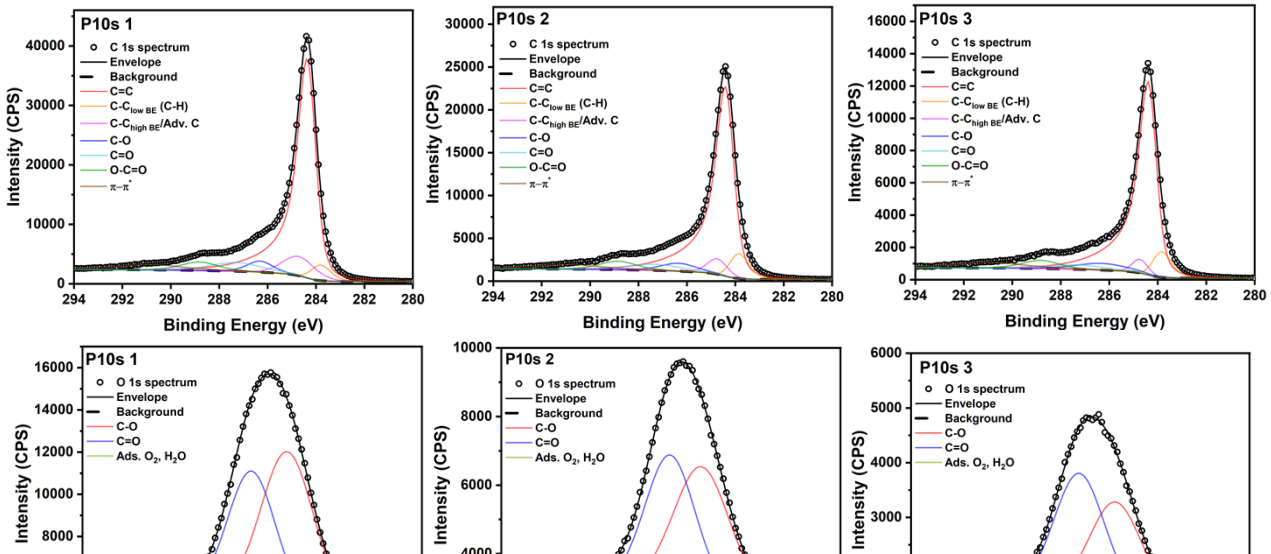

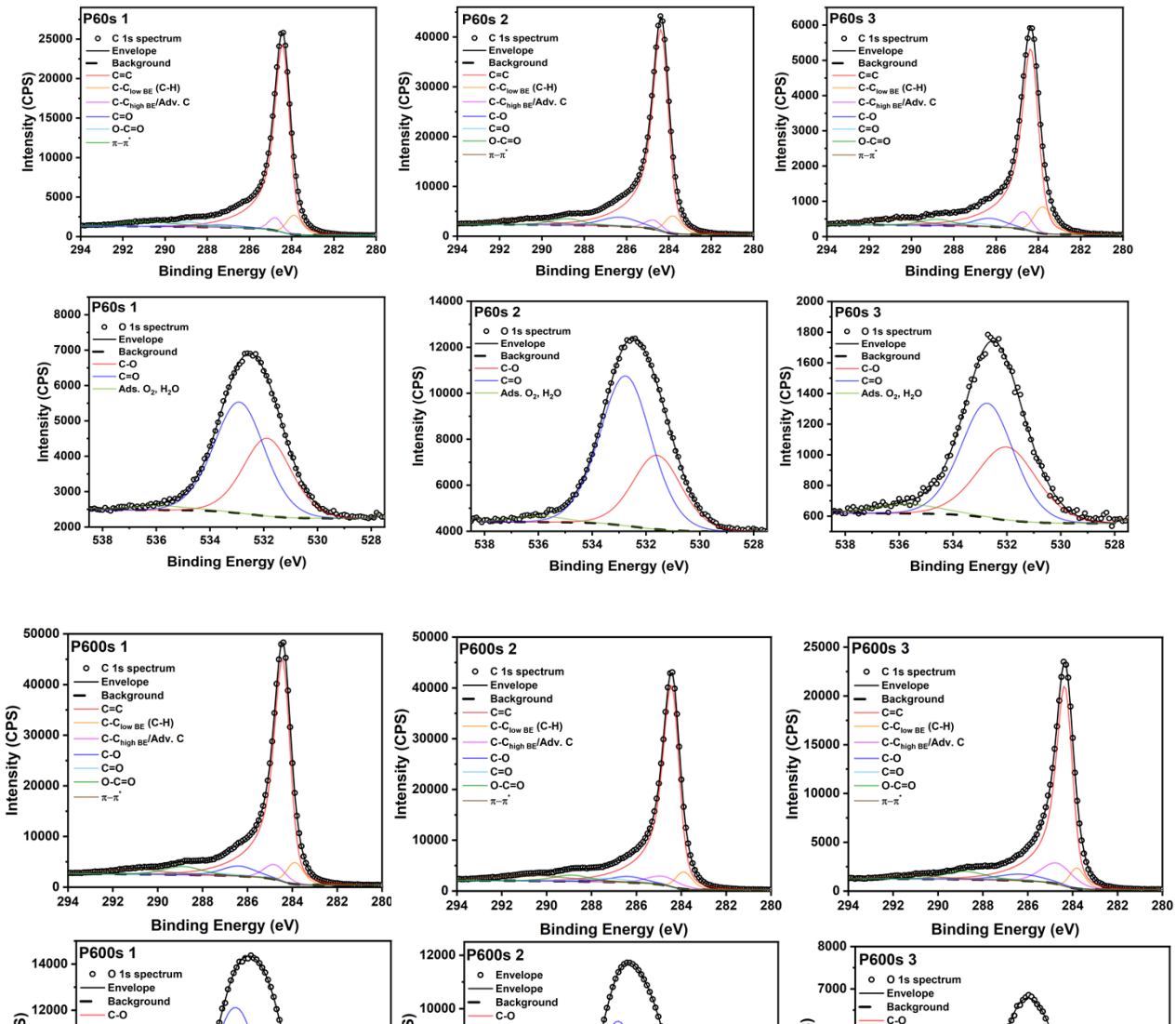
P60s 1
C 1s spectrum
Envelope
Background
C=C
C-C$_{low\ BE}$ (C-H)
C-C$_{high\ BE}$/Adv. C
C=O
O-C=O
π–π*
Intensity (CPS)
Binding Energy (eV)
P60s 2
C 1s spectrum
Envelope
Background
C=C
C-C$_{low\ BE}$ (C-H)
C-C$_{high\ BE}$/Adv. C
C-O
C=O
O-C=O
π–π*
Intensity (CPS)
Binding Energy (eV)
P60s 3
C 1s spectrum
Envelope
Background
C=C
C-C$_{low\ BE}$ (C-H)
C-C$_{high\ BE}$/Adv. C
C-O
C=O
O-C=O
π–π*
Intensity (CPS)
Binding Energy (eV)
P60s 1
O 1s spectrum
Envelope
Background
C-O
C=O
Ads. O$_2$, H$_2$O
Intensity (CPS)
Binding Energy (eV)
P60s 2
O 1s spectrum
Envelope
Background
C-O
C=O
Ads. O$_2$, H$_2$O
Intensity (CPS)
Binding Energy (eV)
P60s 3
O 1s spectrum
Envelope
Background
C-O
C=O
Ads. O$_2$, H$_2$O
Intensity (CPS)
Binding Energy (eV)
P600s 1
C 1s spectrum
Envelope
Background
C=C
C-C$_{low\ BE}$ (C-H)
C-C$_{high\ BE}$/Adv. C
C-O
C=O
O-C=O
π–π*
Intensity (CPS)
Binding Energy (eV)
P600s 2
C 1s spectrum
Envelope
Background
C=C
C-C$_{low\ BE}$ (C-H)
C-C$_{high\ BE}$/Adv. C
C-O
C=O
O-C=O
π–π*
Intensity (CPS)
Binding Energy (eV)
P600s 3
C 1s spectrum
Envelope
Background
C=C
C-C$_{low\ BE}$ (C-H)
C-C$_{high\ BE}$/Adv. C
C-O
C=O
O-C=O
π–π*
Intensity (CPS)
Binding Energy (eV)
P600s 1
O 1s spectrum
Envelope
Background
C-O
Intensity (CPS)
P600s 2
Envelope
Envelope
Background
C-O
Intensity (CPS)
P600s 3
O 1s spectrum
Envelope
Background
C-O
Intensity (CPS)

Raman analysis

Table S2: Gaussian Lorentzian contributions for each band

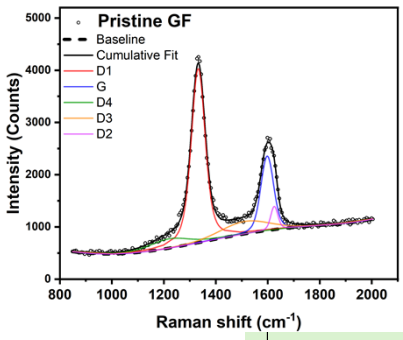

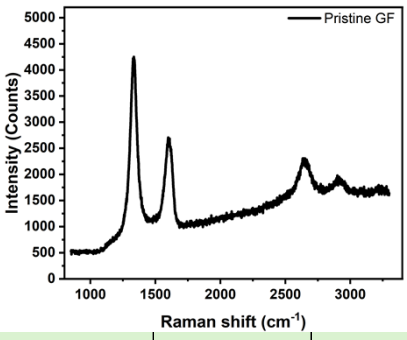

i18		GF400	Id/Ig	3.713565667		P10s	Id/Ig	3.239609023		P60s	Id/Ig	3.283421792	
60		D1 band	Value	Range		D1 band	Value	Range		D1 band	Value	Range	
		Center	1333.94587	1320to1360		Center	1333.57716	1320to1360		Center	1332.5819	1320to1360	
		Area	432141.682			Area	254386.9861			Area	482337.7709		
		wG	39.0275	5-60		wG	40.53759	5-60		wG	36.17939	5-60	
		wL	40	5-40		wL	40	5-40		wL	40	5-40	
		FWHM	**64.62409**			FWHM	**65.99181**			FWHM	**62.07194**		
		Area %	70.70440982			Area %	62.83770222			Area %	69.37630864		
10		Gband				Gband				Gband			
		Center	1599.08449	1580to1610		Center	1599.32798	1580to1610		Center	1598.34704	1580to1610	
		Area	116368.3965			Area	78523.97752			Area	146900.9471		
		Gw	60	5-60		Gw	59.91332	5-60		Gw	60	5-60	
		Lw	6.26352	5-60		Lw	5	5-60		Lw	6.28942	5-60	
		FWHM	**63.41925**			FWHM	**62.6315**			FWHM	**63.43368**		
		Area %	19.03949362			Area %	19.39669317			Area %	21.12927093		
10		D4 band				D4 band				D4 band			
		Center	1210	1190to1210		Center	1210	1190to1210		Center	1210	1190to1210	
		Area	32756.92096			Area	18721.27312			Area	32050.27745		
		Gw	161.39144	50-100		Gw	139.3241	50-200		Gw	129.30389	50-200	
		Lw	5	50-200		Lw	5	50-200		Lw	62.15468	50-200	
		FWHM	**164.08122**			FWHM	**142.01653**			FWHM	**165.72796**		
		Area %	5.3594894			Area %	4.624457421			Area %	4.609902177		
30		D3 band				D3 band				D3 band			
		Center	1513.50276	1510to1530		Center	1510	1510to1530		Center	1510	1510to1530	
		Area	61065.86035			Area	70299.72608			Area	64389.82262		
		Gw	100	5-100		Gw	150	5-150		Gw	100	5-150	
		Lw	100	5-100		Lw	125.89049	5-150		Lw	100	5-150	
		FWHM	**163.75959**			FWHM	**228.3376**			FWHM	**163.75959**		
		Area %	9.991226943			Area %	17.36516998			Area %	9.261410731		
		D2 band				D2 band				D2 band			
		Center	1618.86937	1610to1630		Center	1621.08663	1610to1630		Center	1619.99649	1610to1630	
		Area	38559.83526			Area	11917.99331			Area	36655.05744		
		Gw	39.04722	5-50		Gw	34.25234	5-50		Gw	37.40419	5-50	
		Lw	5	5-50		Lw	5	5-50		Lw	5	5-50	
		FWHM	**41.7895**			FWHM	**37.0043**			FWHM	**40.14951**		
		Area %	6.308927161			Area %	2.943937212			Area %	5.272223598		

Pristine	Id/Ig	2
D1 band	Value	
Center	1332.14763	
Area	289903.8301	
wG	36.80391	
wL	40	
FWHM	**62.62825**	
Area %	65.51077466	
Gband		
Center	1599.62903	
Area	108176.8039	
Gw	59.63946	
Lw	8.90526	
FWHM	**64.54405**	
Area %	24.44516246	
D4 band		
Center	1210	
Area	28893.98248	
Gw	57.69697	
Lw	200	
FWHM	**216.43228**	
Area %	6.529293436	
D3 band		
Center	1510	
Area	42824.71936	
Gw	100	
Lw	100	
FWHM	**163.75959**	
Area %	9.677280009	
D2 band		
Center	1623.11865	1610to1630
Area	10482.65493	
Gw	29.99223	5-50
Lw	5	5-50
FWHM	**32.75537**	
Area %	2.368809148	

Figure S7: Pristine **GF** Raman spectrum and D/G band deconvolution.

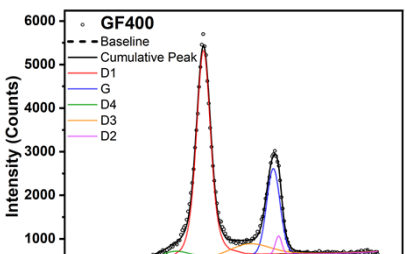

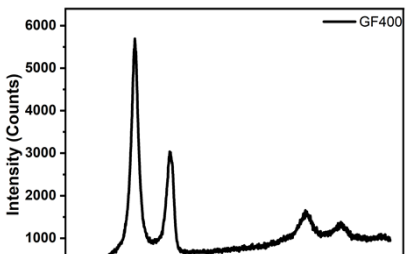

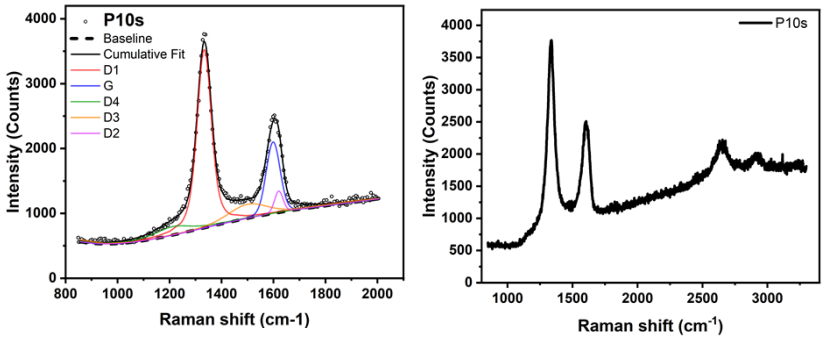

Figure S9: **P10s** Raman spectrum and D/G band deconvolution.

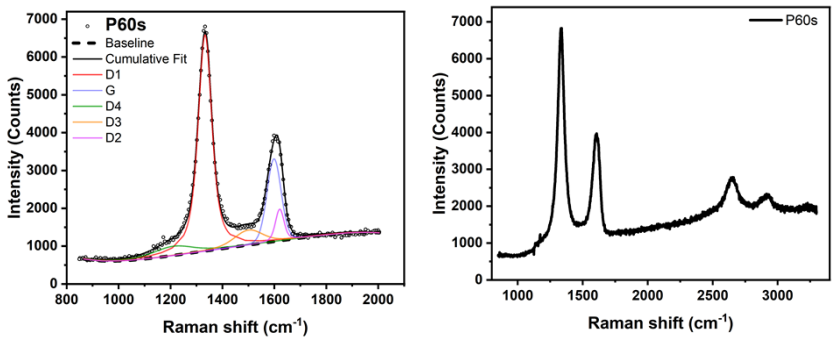

Figure S10: **P60s** Raman spectrum and D/G band deconvolution.

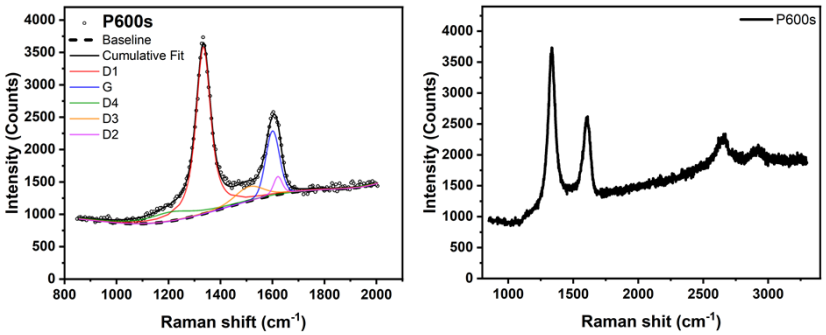

Figure S11: **P600s** Raman spectrum and D/G band deconvolution.

Electrochemical double layer capacitance analysis

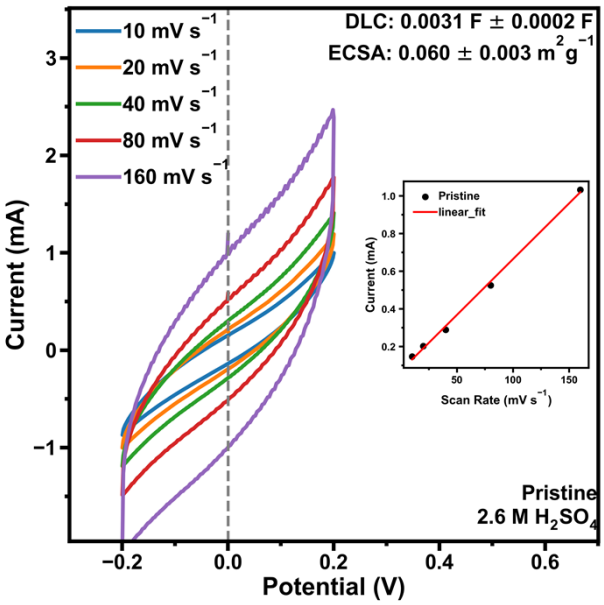

Figure S12: Pristine **GF** cyclic voltammetry showcasing non-faradaic current at different scan rates and linear fit of a current vs scan rate plot.

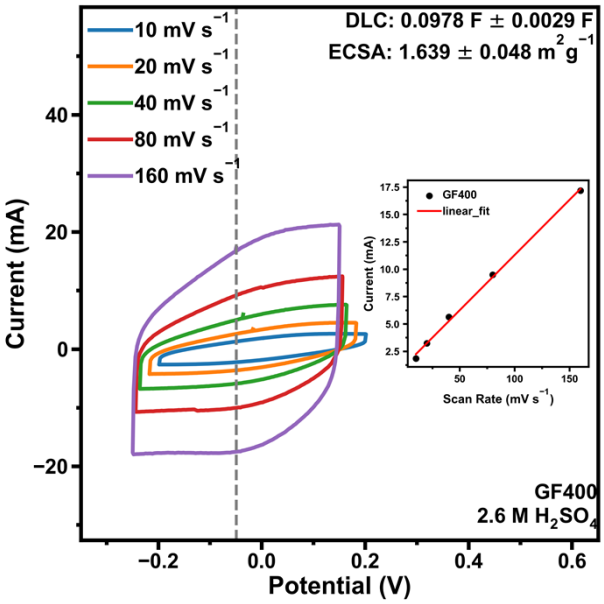

Figure S13: **GF400** cyclic voltammetry showcasing non-faradaic current at different scan rates and linear fit of a current vs scan rate plot.

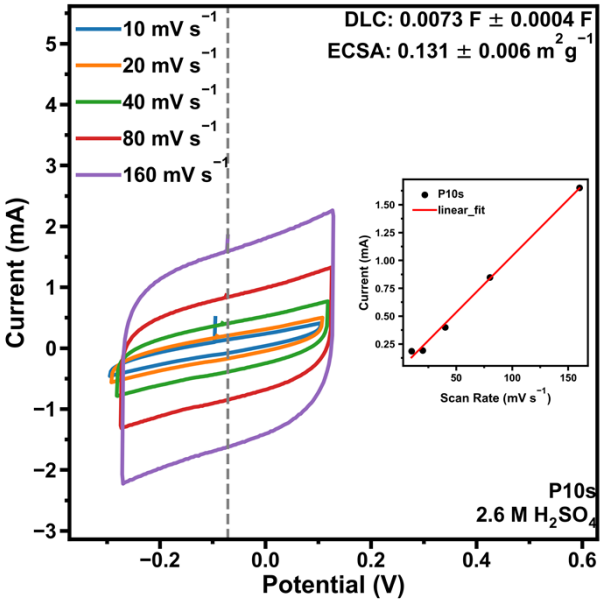

Figure S14: **P10s** cyclic voltammetry showcasing non-faradaic current at different scan rates and linear fit of a current vs scan rate plot.

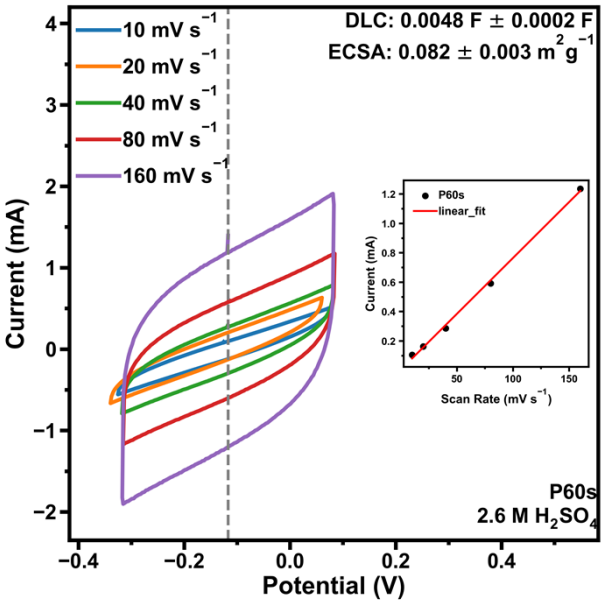

Figure S15: **P60s** cyclic voltammetry showcasing non-faradaic current at different scan rates and linear fit of a current vs scan rate plot.

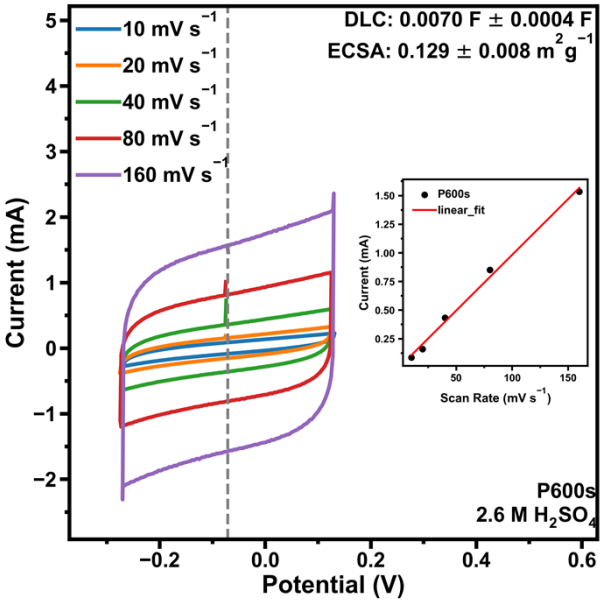

Figure 16: **P60s** cyclic voltammetry showcasing non-faradaic current at different scan rates and linear fit of a current vs scan rate plot.

BET analysis.

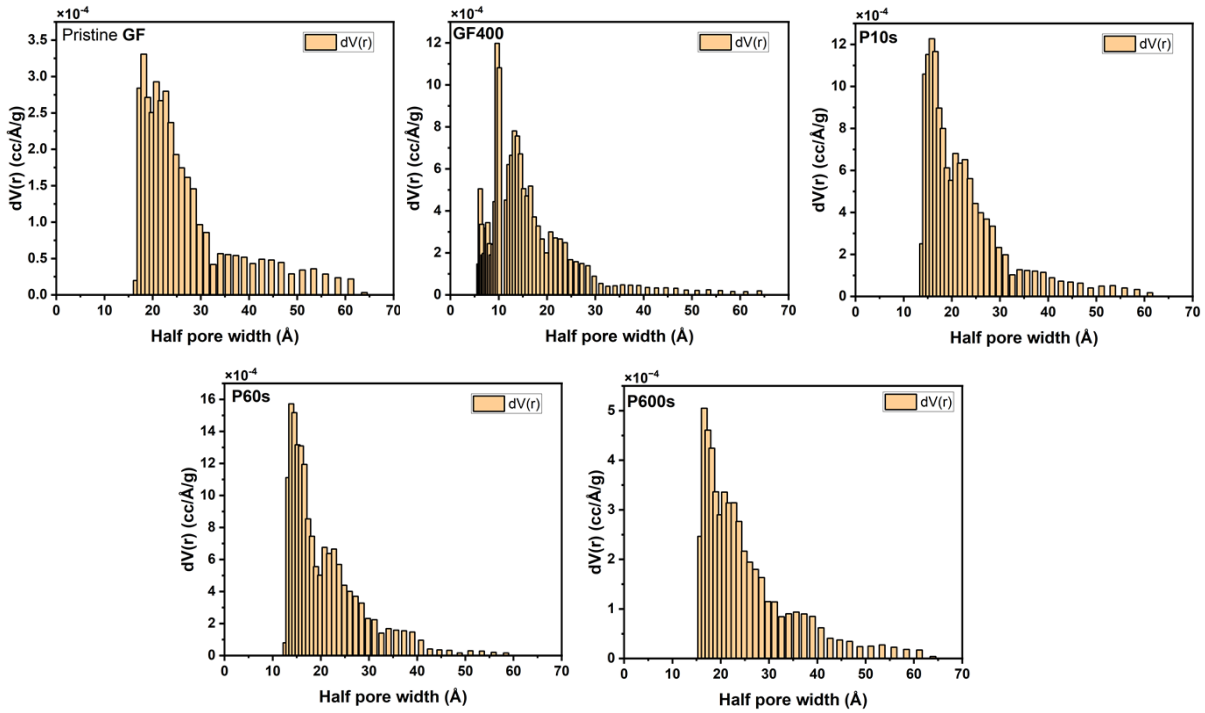

Figure S17: Pore-size distributions from electrodes as derived from BET analysis.

Single-electrolyte cell analysis.

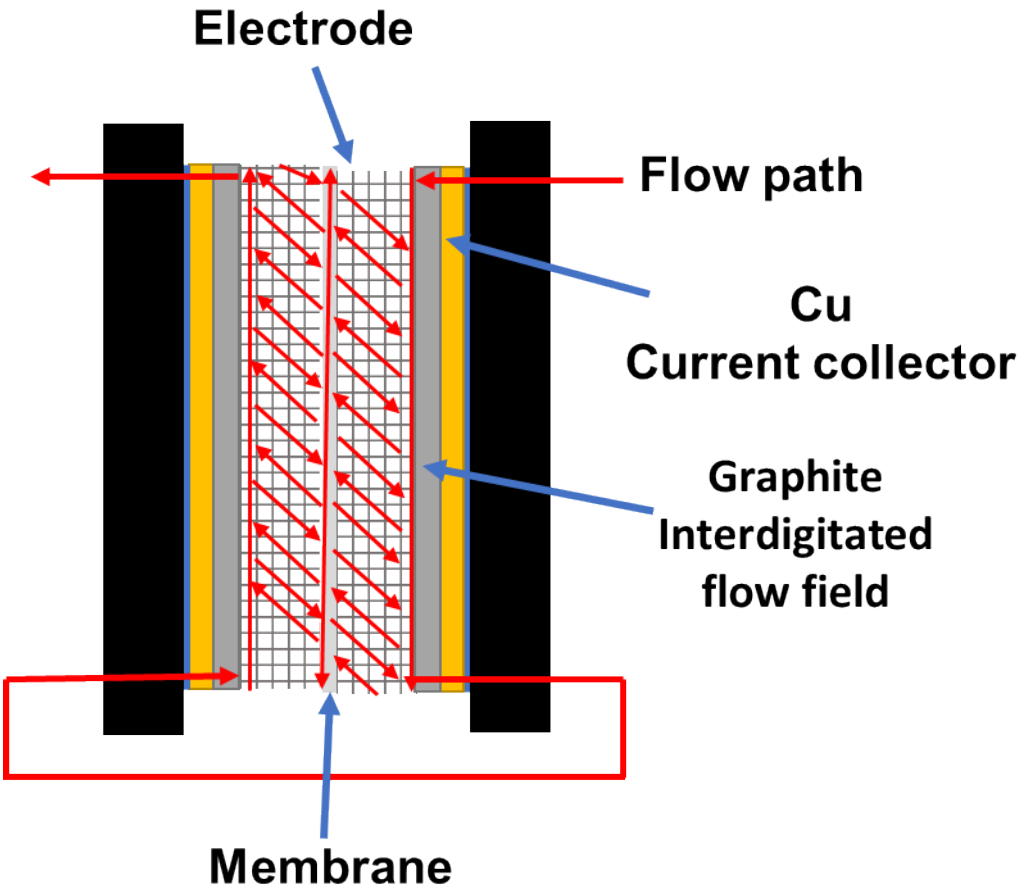

Figure S18: Schematic of a Single-electrolyte flow cell.

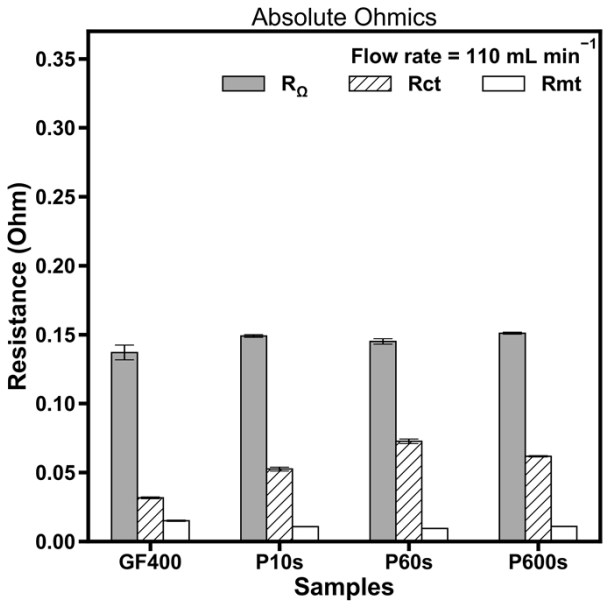

Figure S19: Breakdown of impedance contributions: Ohmic resistance (Rs), charge-transfer resistance (Rct) and mass-transport resistance (Rmt) at 110 mL min^{-1}

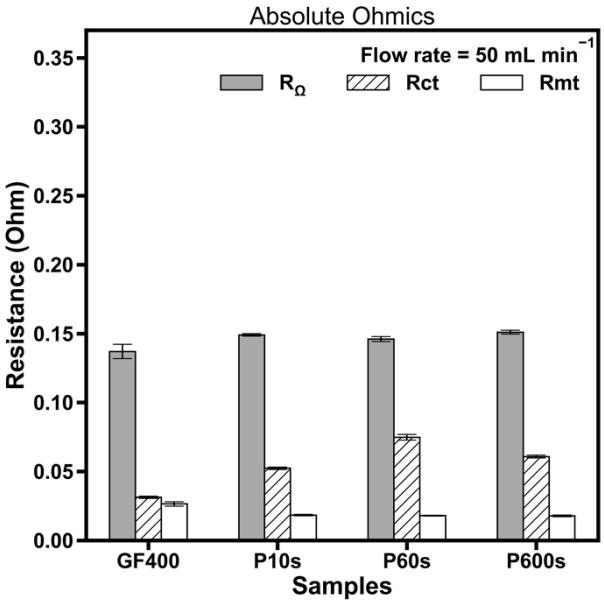

Figure S20: Breakdown of impedance contributions: Ohmic resistance (Rs), charge-transfer resistance (Rct) and mass-transport resistance (Rmt) at 50 mL min^{-1}

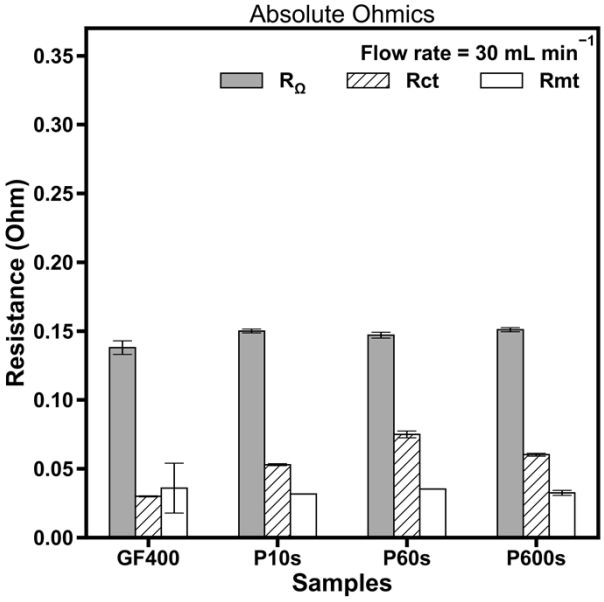

Figure S21: Breakdown of impedance contributions: Ohmic resistance (Rs), charge-transfer resistance (Rct) and mass-transport resistance (Rmt) at 30 mL min^{-1}

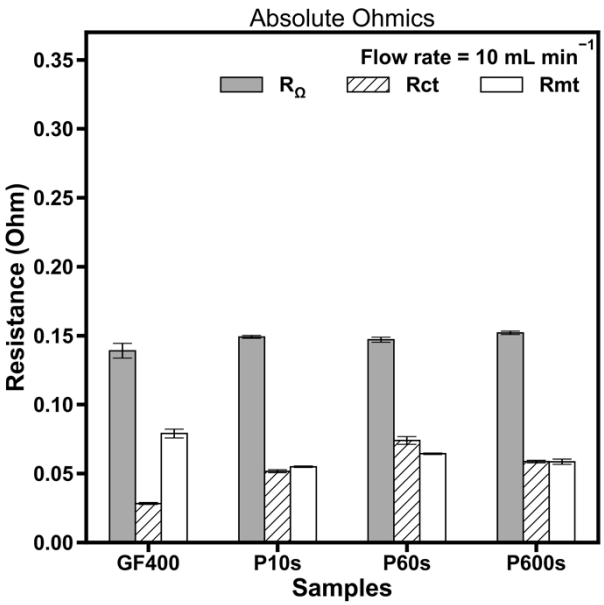

Figure S22: Breakdown of impedance contributions: Ohmic resistance (Rs), charge-transfer resistance (Rct) and mass-transport resistance (Rmt) at 10 mL min^{-1}

Pressure drop analysis.

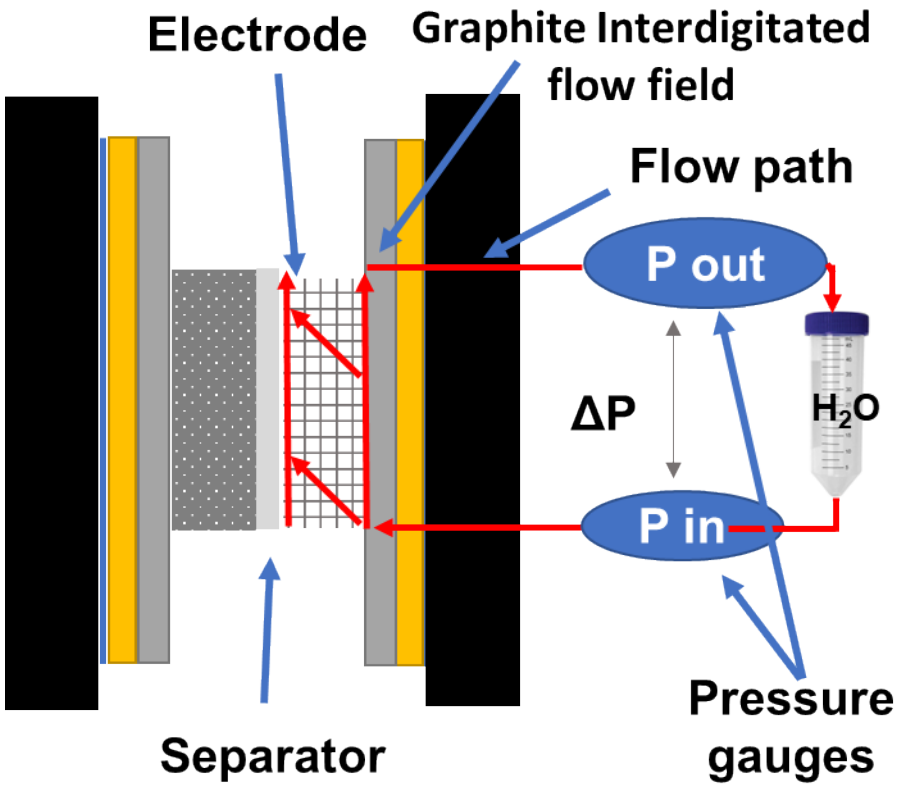

Figure S23: Schematic of a Flow cell set up to perform pressure drop measurements.

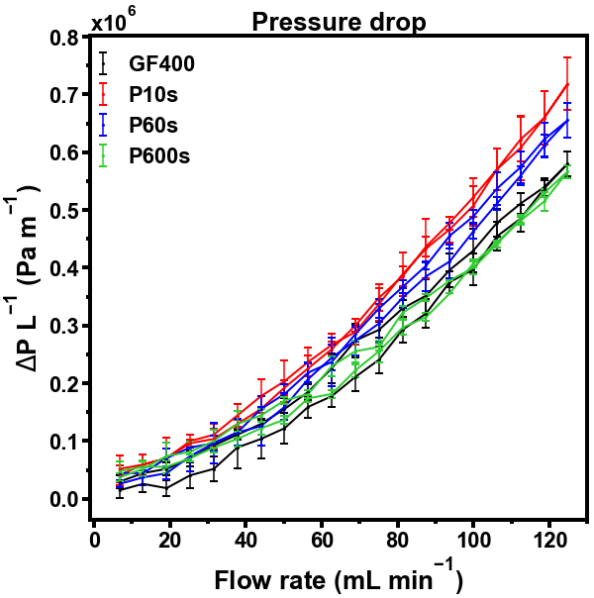

Figure S24: Pressure drop plot from different electrodes showcasing curve hysteresis.

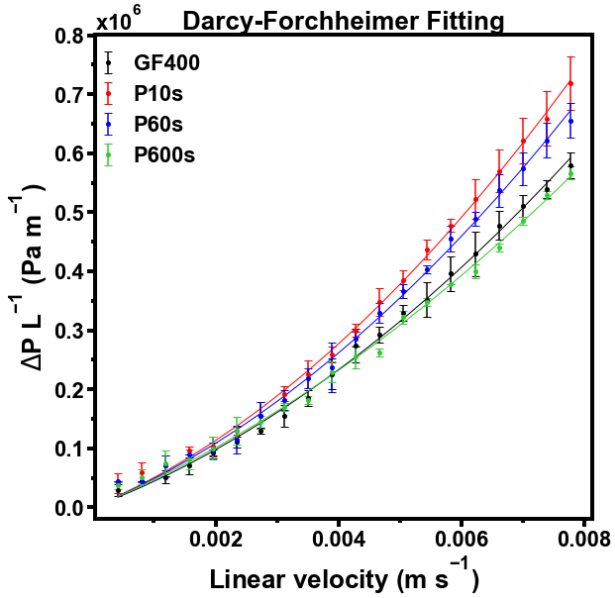

Figure S25: Darcy-Forchheimer fitting.

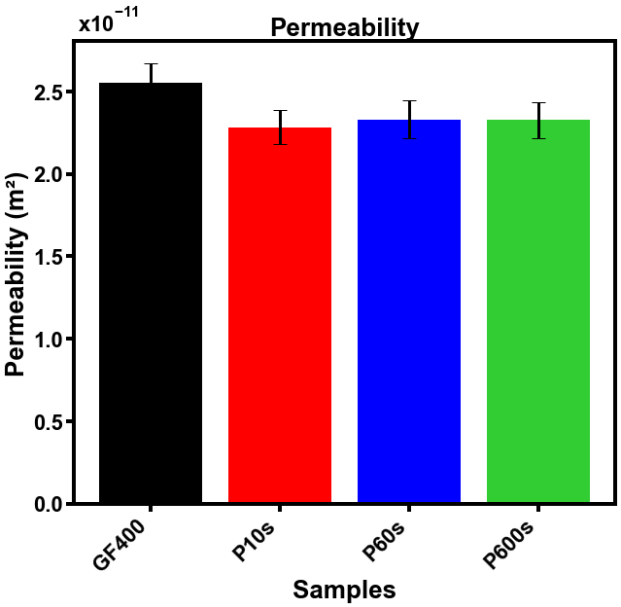

Figure S26: Permeability values derived from Darcy-Forchheimer fitting